

## ESR STUDY OF SOLVENT EFFECTS ON THE ELECTRONIC STRUCTURE OF 2-(4'-DIALKYLAMINOPHENYL)INDAN-1,3-DIONYL RADICALS

YOSHIMI SUEISHI\*, TAKANORI ISOZAKI, SHUNZO YAMAMOTO AND NORIO NISHIMURA

*Department of Chemistry, Faculty of Science, University of Okayama, Tsushima, Okayama, 700 Japan*

The ESR spectra of 2-arylindan-1,3-dionyl radicals in various solvents at 343 K were obtained and assignments of the hyperfine structures were made. The hyperfine coupling constant (hfcc) of the dimethylamino nitrogen increases whereas the 2',6'-hydrogen hfcc decreases as the  $E_T$  value, a solvent polarity parameter, increases. MO calculations were made according to the semi-empirical procedure of Rieger and Fraenkel; the nitrogen and oxygen Coulomb integrals were adjusted so that the calculated spin density on the nitrogen atom agrees with that estimated from its hfcc. It is found that the  $\pi$ -moment of the radicals increases from 9.13 D in toluene to 9.85 D in acetic acid. The solvent dependence of the equilibrium between the radicals and its dimer has been explained in terms of the solvent-induced  $\pi$ -moment in polar solvents.

### INTRODUCTION

From recent studies of solvent effects in chemical kinetics and equilibria, it has been clarified that the change in the solvent-induced solute dipole moment plays an important role. For example, Abdel-Mottaleb and Abdel-Kaker<sup>1</sup> examined the solvent-induced change in the electronic structure of conjugation systems on the basis of the <sup>1</sup>H NMR spectral shifts in various solvents. They considered that the spectral shifts are regarded as a good indication of the change in electronic structure. Botrel *et al.*<sup>2</sup> applied the CNDO/SCI method to so-called push-pull molecules. They also pointed out the significant increase in the solute dipole moment with increasing solvent polarity. Previously, we studied the effects of pressure and solvent on the rate of thermal isomerizations of push-pull azobenzenes<sup>3</sup> and 6-nitrospiroyan,<sup>4</sup> and interpreted the effects in terms of solvent-induced changes in the electronic structures.

Mukai *et al.*<sup>5</sup> studied the variation of nitrogen hfcc in diphenyl nitroxide with solvents. They suggested that the surrounding solvents cause redistribution of the  $\pi$ -electrons. Poluektov *et al.*<sup>6</sup> observed the poorly resolved ESR spectrum of 2-(4'-dimethylaminophenyl)-indan-1,3-dionyl radical (**1a**) produced on heating the dimer of **1a** to 343 K. Since **1a** possesses a push-pull electronic character, it would be stabilized by polar solvents.

This study was aimed at examining how solvents affect the ESR spectra of 2-(4'-dialkylaminophenyl)-indan-1,3-dionyl radicals.

### EXPERIMENTAL

The dimer (**D**) of 2-(4'-dimethylaminophenyl)indan-1,3-dionyl radical (**1a**) was prepared according to the method of Karele and Neiland<sup>7</sup> and recrystallized from acetone-water: m.p. 216–217 °C (lit.<sup>7</sup> m.p., 216–217 °C). The dimer of 2-(4'-diethylaminophenyl)-indan-1,3-dionyl radical (**11a**) was obtained by the modified procedure of Beringer *et al.*<sup>8</sup> and recrystallized from ethanol-chloroform: m.p. 201–203 °C (lit.<sup>7</sup> m.p., 207–208 °C). Melting point, IR and <sup>1</sup>H NMR spectra were used for identification. Solvents of reagent grade were stored over molecular sieves and distilled just before use.

ESR spectra were recorded on a JEOL FE-3XG X-band spectrometer equipped with a 100 kHz field modulation. Dissolved oxygen in a dimer solution (*ca* 10<sup>-2</sup> mol dm<sup>-3</sup>) was removed by the freeze-thaw method. Temperature was controlled using a JEOL variable-temperature regulator. Spectral simulation was made with an attached computer (DEC RT-11). The concentration of **1a** was determined by double integration of the first-derivative signal with the aid of an attached computer program, using 2,2-diphenyl-1-picrylhydrazyl as a standard.

\* Author for correspondence

## RESULTS AND DISCUSSION

## Solvent effects on ESR spectra

The equilibrium between arylindandionyl radicals ( $R\cdot$ ) and its dimer ( $D$ ) is expressed as<sup>6,9</sup>



This equilibrium is favourable for the dimer at room temperature. With increasing temperature, the dimer dissociates to the radicals and the intensity of the ESR spectra increases. We obtained the well resolved ESR spectra of **1a** at 343 K in various solvents and representative spectra are shown in Figures 1(a) and 2(a). The nitrogen and hydrogen hyperfine coupling constants (hfccs) ( $a_N$  and  $a_H$ ) of **1a** in carbon tetrachloride, chloroform, 1,2-dichloroethane and acetonitrile were determined by the simulation technique, referring to the calculated spin densities (see below). The  $a_N$ ,  $a_H^{CH_3}$  and  $a_H^{2,6}$  values in dioxane, toluene, acetophenone, *N,N*-dimethylformamide and dimethyl sulphoxide were estimated directly. The estimated hfcc values are given in Table 1. Figures 1(b) and 2(b) represent the simulated signals. Figure 3 shows the relationship between the nitrogen and hydrogen hfccs and the  $E_T$  value (solvent polarity parameter). Knauer and Napier<sup>10</sup> showed that the  $a_N$  values of nitroxides are correlated well with solvent polarity parameters such as the  $E_T$  and  $Z$  values.

For **1a**, various kinds of canonical resonance forms can be written as depicted in Scheme 1. The increase in the nitrogen hfcc means an increase in the spin density

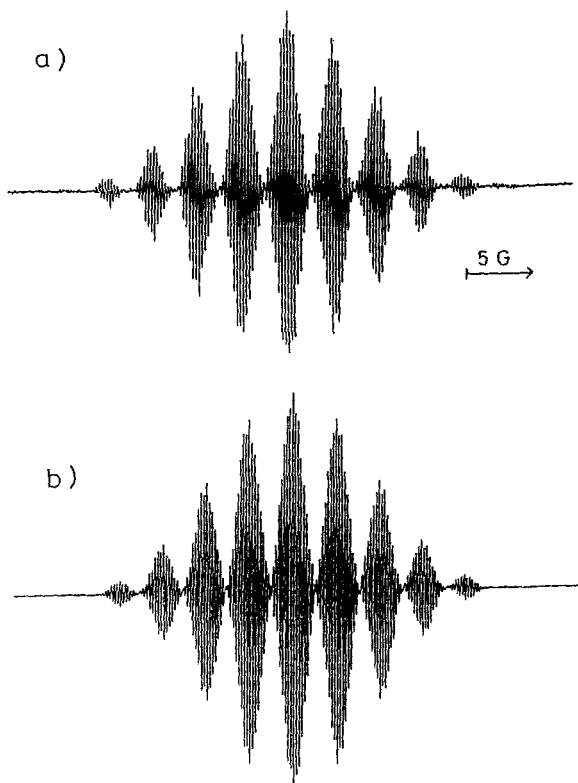


Figure 1. (a) ESR spectrum of **1a** in  $CCl_4$  at 343 K; (b) computer-simulated spectrum

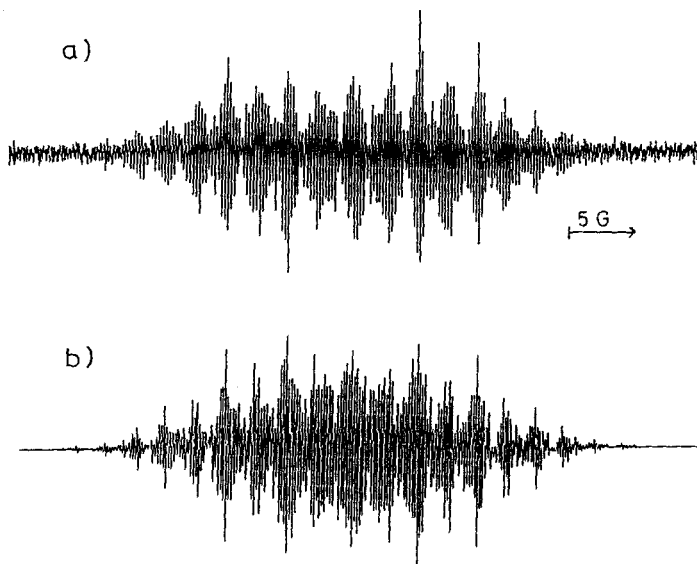
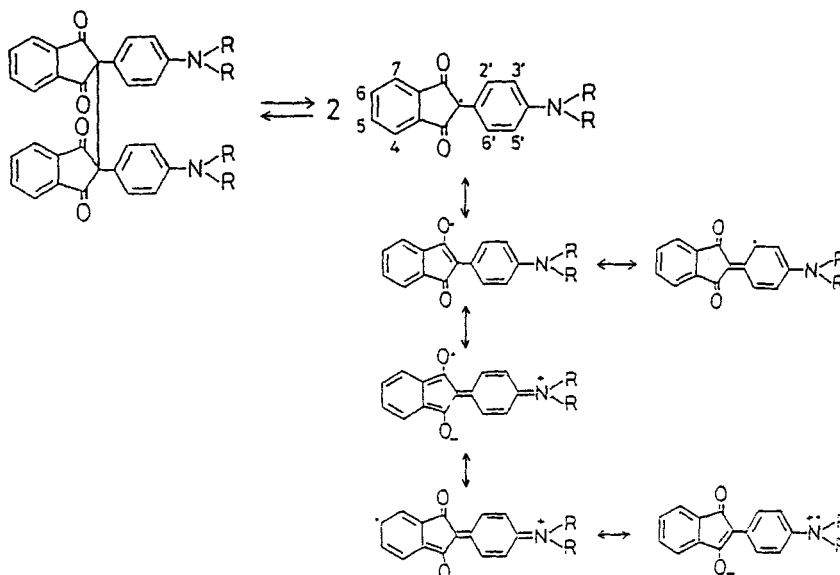


Figure 2. (a) ESR spectrum of **1a** in acetonitrile at 343 K; (b) computer-simulated spectrum

Table 1. Hyperfine coupling constants of nitrogen and hydrogen (in G<sup>a</sup>) for **Ia** and **IIa** in various solvents<sup>b</sup> at 343 K

Compound	Parameter	CCl <sub>4</sub>	Toluene	Dioxane	CHCl <sub>3</sub>	DE	AP	DMF	DMSO	CH <sub>3</sub> CN
<b>Ia</b>	$\lambda_{\max}$	680	703	710	718	723	733	738	746	730
	$a_N$	3.61	3.92	4.10	4.15	4.38	4.56	4.86	5.06	4.72
	$a_{\text{CH}_3}$	3.17	3.47	3.61	3.73	3.89	4.08	4.44	4.67	4.29
	$a_{\text{H}^{6'}}$	2.72	2.50	2.92	2.31	2.22	2.16	1.94	1.83	2.06
	$a_{\text{H}^{3',5'}}$	0.67			0.70	0.54				0.95
	$a_{\text{H}^{6'}}$	0.43			0.54	0.46				0.36
	$a_{\text{H}^{4'7'}}$	0.25			0.23	0.24				0.22
	$a_N (= 2a_{\text{H}^{3'6'}} = 2a_{\text{H}^{2',6'}})$	3.8	4.1	4.6	4.4	4.4		5.3		4.9
<b>IIa</b>										

<sup>a</sup>  $1G \approx 0.1 \text{ mT}$ .<sup>b</sup> DE = 1,2-dichloroethane; AP = acetophenone; DMF = *N,N*-dimethylformamide; DMSO = dimethyl sulphoxide.



Scheme 1

on it. As expected, the absorption band of **1a** in the visible region is also sensitive to solvent polarity (Table 1). We have already reported a similar trend for push-pull molecules<sup>3,4</sup> and quinazoliyloxyl radical.<sup>11</sup>

The ESR spectra of **IIa** in toluene, 1,2-dichloroethane and acetonitrile are shown in Figure 4. The ESR signals consist of 11 equidistant lines. Poluektov *et al.*<sup>6</sup> have ascribed the hfs to nitrogen, four equivalent hydrogens of methylene groups and two equivalent hydrogens of the phenyl ring, assuming that

the magnitude of hydrogen hfccs is just half that of nitrogen hfcc:  $a_N \approx 2a_H^{CH_2} \approx 2a_H^{2,6'}$ . The additional incomplete splitting of each line shows small differences in the hfccs of these hydrogen groups and/or the participation of other hydrogens. The nitrogen hfccs for **IIa** in various solvents are given in Table 1. It should

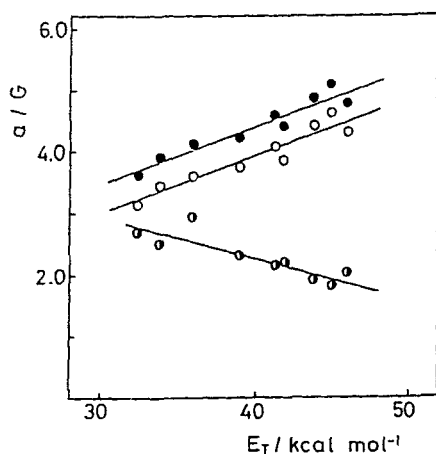


Figure 3. Relationship between the nitrogen and hydrogen coupling constants and  $E_T$  values for **Ia**. (●)  $a_N$ ; (○)  $a_H^{CH_3}$ ; (◐)  $a_H^{2,6'}$ .

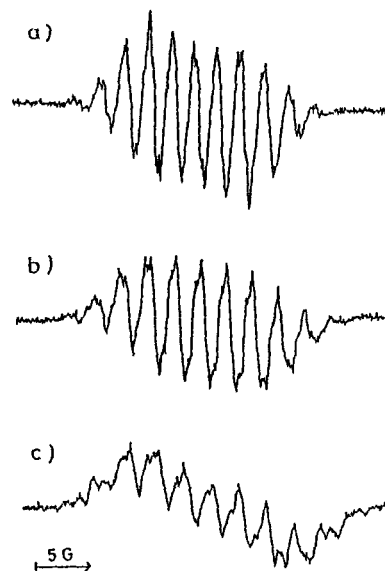


Figure 4. ESR spectra of **IIa** at 343 K: (a) in toluene; (b) in 1,2-dichloroethane; (c) in acetonitrile

be noted that the  $a_{\text{H}}^{\text{CH}_2}$  value for each solvent is about half that of  $a_{\text{H}}^{\text{CH}_3}$  for **1a**. Abakumov *et al.*<sup>12</sup> reported similar results for dialkylaminophenoxyl radicals, attributing the barrier to rotation about the  $\text{C}_{\text{alkyl}}-\text{N}$  bond. The dependence of the nitrogen hfcc for **1a** on the  $E_{\text{T}}$  value is similar to the values observed for **1a**.

### Estimation of spin density

The  $\pi$ -electron spin density in aromatic compounds can be estimated by the following empirical relationship:<sup>13</sup>

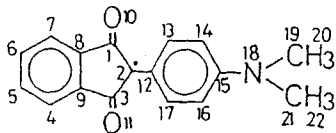
$$a_{\text{H}}^i = Q_{\text{CH}} \rho_i \quad (2)$$

where  $a_{\text{H}}^i$  denotes the hfcc for the hydrogen bonded to the  $i$ -th carbon atom,  $\rho_i$  is the  $\pi$ -electron spin density on the carbon atom and  $Q_{\text{CH}}$  is a constant, a value of  $22.5 \text{ G}$ <sup>14</sup> usually being used. A similar relationship is used for nitrogen and the  $Q_{\text{N}}$  value is  $21.1 \text{ G}$ <sup>15</sup>. The spin densities ( $\rho_{\text{N}}$  and  $\rho_{\text{C}}^{2,6'}$ ) calculated by equation (2) are plotted against  $E_{\text{T}}$  in Figure 5.

Rieger and Fraenkel<sup>16</sup> performed molecular orbital (MO) calculations for nitro-substituted aromatic anion radicals using the Hückel LCAO theory combined with McLachlan's approximate configuration-interaction method. They showed that if the Coulomb integrals the nitrogen and oxygen are properly chosen from solvent to solvent, the calculated spin densities on the nitrogen and carbon atoms for the nitrobenzene anion radicals are well correlated with those estimated from experimental hfccs.

We have carried out similar MO calculations for **1a**. The integral parameters required for the MO calculations are given by the equation  $\alpha_{\text{X}} = \alpha + \delta_{\text{X}}\beta$ , where  $\alpha$  and  $\beta$  are the Coulomb and resonance integrals for benzene, respectively,  $\alpha_{\text{X}}$  is the Coulomb integral for atom X, and  $\delta_{\text{X}}$  is the empirical parameter. At first, the MO calculations for **1a** were made to fit the spin densities in  $\text{CCl}_4$  with a proper choice of the parameters. As a result of trial-and-error, we adopted the values  $\delta_{\text{N}} = 0.595$  and  $\delta_{\text{O}} = 1.42$  for **1a** in  $\text{CCl}_4$ . The spin densities calculated by using these parameters are  $\rho_{\text{N}} = 0.1796$ ,  $\rho_{\text{C}}^{2,6'} = 0.1031$  and  $\rho_{\text{C}}^{3',5'} = 0.0223$ ,\* which

\* The following parameters were used for the calculations.<sup>16,17</sup>



$$\begin{aligned} \alpha_{19} &= \alpha_{21} = \alpha - 0.1\beta, \quad \alpha_{20} = \alpha_{22} = \alpha - 0.5\beta, \\ \beta_{1,2} &= \beta_{2,3} = \beta_{1,8} = \beta_{3,9} = 0.9\beta, \quad \beta_{15,18} = \beta_{18,19} = \beta_{18,21} = 0.8\beta, \\ \beta_{19,20} &= \beta_{21,22} = 3\beta. \end{aligned}$$

When resonance integrals  $\beta_{1,10} = \beta_{3,11} = 2.6\beta$  were chosen, the spin densities calculated by the Hückel MO best agreed with the experimental values.

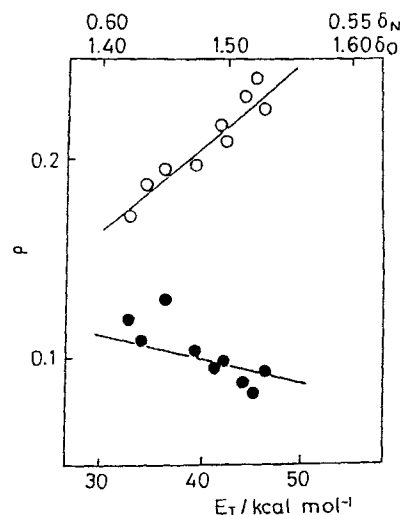


Figure 5. Plots of the spin densities on the nitrogen atom ( $\circ$ ) and the carbon atoms at 2',6'-positions ( $\bullet$ ) as a function of  $E_{\text{T}}$  values. Solid lines represent the spin density calculated as a function of the Coulomb integral parameters for the oxygen ( $\delta_{\text{O}}$ ) and nitrogen ( $\delta_{\text{N}}$ ) atoms of **1a**

are in good agreement with those estimated according to equation (2) ( $\rho_{\text{N}} = 0.171$ ,  $\rho_{\text{C}}^{2,6'} = 0.121$  and  $\rho_{\text{C}}^{3',5'} = 0.030$ ). A set of Coulomb integrals for the nitrogen and oxygen (1.40–1.56 for the oxygen and 0.60–0.56 for the nitrogen) was chosen so that the calculated spin densities on the nitrogen for each solvent reproduce those estimated by equation (2) (Figure 5). Using these Coulomb integrals, the spin densities on the 2',6'-carbon atoms were calculated. It should be noted that the lower solid line in Fig. 5 has a negative slope and passes through the experimentally estimated points.

### Solvent Effects on equilibrium constants

The equilibrium constant  $K$  between arylindandionyl radical ( $\text{R}\cdot$ ) and its dimer ( $\text{D}$ ) is expressed by

$$K = [\text{R}\cdot]^2 / [\text{D}] = 2[\text{R}\cdot]^2 / (2[\text{D}]_0 - [\text{R}\cdot]) \quad (3)$$

where  $[\text{D}]$  and  $[\text{R}\cdot]$  are the concentrations of the dimer and the radical at equilibrium, respectively, and  $[\text{D}]_0$  denotes the initial concentration of the dimer. The  $K$  value estimated by means of ESR method at 323 K in toluene, 1,2-dichloroethane, acetone and acetonitrile are given in Table 2. The estimation of the radical concentration in the remaining solvents was unsuccessful owing to technical difficulties. The equilibrium constants in toluene, chloroform, 1,1,2,2-tetrachloroethane,  $N,N$ -dimethylformamide and acetic acid at 323 K were calculated from the reported enthalpy ( $\Delta H$ ) and entropy ( $\Delta S$ ) changes for the radical-dimer equilibrium.<sup>9</sup> It can be seen from the

Table 2. Calculated  $\pi$ -moments of **1a** and equilibrium constants in various solvents at 323 K

No.	Solvent	$E_T$ (kcal mol <sup>-1</sup> )	$\left(\frac{\epsilon-1}{2\epsilon+1}\right)^a$	$\mu(\pi)$ (D)	$10^9 K$ (mol dm <sup>-3</sup> ) <sup>b</sup>
1	Toluene	33.9	0.240	9.13	0.741 (0.492)
2	Chloroform	39.1	0.356	9.34	(2.51)
3	1,1,2,2-Tetrachloroethane		0.414		(8.53)
4	1,2-Dichloroethane	41.9	0.433	9.45	41.7
5	Acetone	42.2	0.465	9.46	23.1
6	<i>N,N</i> -Dimethylformamide	43.8	0.480	9.52	(9.85)
7	Acetonitrile	46.0	0.480	9.61	68.5
8	Acetic acid	51.9	0.388	9.85	(6.71)

<sup>a</sup> Dielectric constants at 298 K were used.<sup>b</sup> The presumed equilibrium constants are given in parentheses (see text).

that the equilibrium constants generally tend to increase with increasing solvent polarity.

On the basis of the Kirkwood treatment,<sup>18</sup> the dielectric influence of solvents on the equilibrium constants is given by

$$\ln K = \ln K_0 + (N/RT) [(2\mu_R^2/r_R^3) - (\mu_D^2/r_D^3)] (\epsilon - 1) / (2\epsilon + 1) \quad (4)$$

where  $\mu_R$  and  $\mu_D$  are the dipole moments of the radical and the dimer, respectively. Equation (4) predicts a linear relationship between  $\ln K$  and  $(\epsilon - 1)/(2\epsilon + 1)$  with a slope of  $(N/RT) [(2\mu_R^2/r_R^3) - (\mu_D^2/r_D^3)]$ . Figure 6(a) shows the Kirkwood plots using the data in Table 2. It can be seen that the plots deviate upwards as  $(\epsilon - 1)/(2\epsilon + 1)$  increases. We reported previously such a non-linear behaviour of the Kirkwood plot for the isomerization of push-pull azobenzenes<sup>3</sup> and spiropyrans,<sup>4</sup> and suggested that this arises from the neglect of the enhanced polarization in polar solvents.

Using the empirically determined parameters in the above procedure, the  $\pi$ -moments of **1a** in several solvents can be calculated from the charge densities and they are given in Table 2. As expected, the  $\pi$ -moments are larger in media with higher  $E_T$  values. With the aid of the Corey-Pauling-Kolton (CPK) model, the hydrodynamically equivalent approximate radii of the dimer and the radical were estimated to be  $r_D = 5.5$  and  $r_R = 3.5$  Å, respectively. From a plausible torsion of dimer moieties, we roughly assumed the dipole moment of the dimer to be  $\mu_D = 3$  D without explicit evidence. Owing to the approximate nature of the Kirkwood treatment, we tentatively used the value of the  $\pi$ -moment instead of the total dipole moment ( $\pi + \sigma$ ). In Figure 6(b),  $\ln K$  is plotted against  $[(2\mu_R^2/r_R^3) - (\mu_D^2/r_D^3)] (\epsilon - 1)/(2\epsilon + 1)$ . Although a considerable scatter is observed, the linearity is improved. Equation (4) predicts that the slope of the plot should be  $N/RT$  ( $= 2 \times 10^{20}$  J<sup>-1</sup>), but the actual slope is  $0.4 \times 10^{20}$  J<sup>-1</sup>. Owing to the approximate nature of the above treatment, the agreement could be said to be fair.

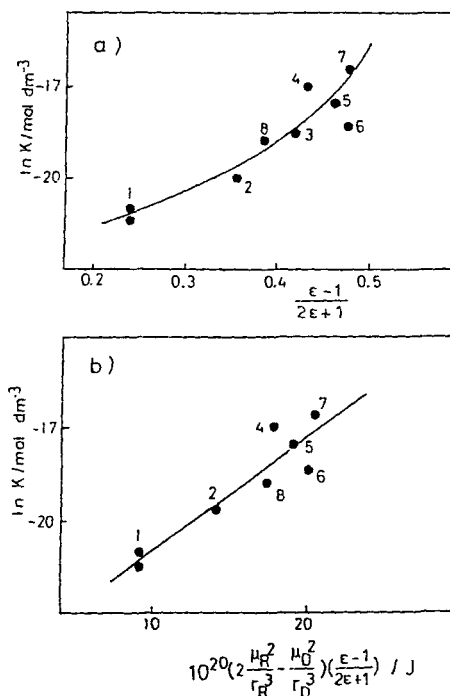


Figure 6. (a)  $\ln K$  vs  $(\epsilon - 1)/(2\epsilon + 1)$  relationship for the dimer-radical equilibrium at 323 K. (b)  $\ln K$  vs  $[(2\mu_R^2/r_R^3) - (\mu_D^2/r_D^3)] (\epsilon - 1)/(2\epsilon + 1)$  plot. For numbering, see Table 2

In conclusion, the all above findings clearly show that solvent-induced polarization plays an important role.

## REFERENCES

1. M. S. A. Abdel-Mottaleb and M. N. Abdel-Kader, *Indian J. Chem.* **22B**, 1217 (1983).

2. A. Botrel, A. Le Beuze, P. Jacques and H. Strub, *J. Chem. Soc., Faraday Trans. 2* **80**, 1235 (1984).
3. N. Nishimura, S. Kosako and Y. Sueishi, *Bull. Chem. Soc. Jpn.* **57**, 1617 (1984); N. Nishimura, T. Tanaka, M. Asana and Y. Sueishi, *J. Chem. Soc., Perkin Trans. 2* 1839 (1984).
4. Y. Sueishi, M. Ohcho and N. Nishimura, *Bull. Chem. Soc. Jpn.* **58**, 2608 (1985).
5. K. Mukai, H. Nishiguchi, K. Ishizu and Y. Deguchi, *Bull. Chem. Soc. Jpn.* **40**, 2731 (1967).
6. I. T. Poluektov, V. V. Moiseev, I. F. Gainulin and A. I. Yasumenko, *Zh. Org. Khim.* **11**, 1300 (1975).
7. B. Ya. Karele and O. Ya. Neiland, *Izv. Akad. Latv. SSR, Ser. Khim.* 599 (1964).
8. F. M. Beringer, S. A. Galton and S. J. Huang, *Tetrahedron* **19**, 809 (1963).
9. I. V. Khudyakov, V. A. Kuzumin, A. I. Yasmenko, W. Smit, J. Salve and C. R. H. I. DE Jong, *Int. J. Chem. Kinet.* **16**, 1481 (1984).
10. B. R. Knauer and J. J. Napier, *J. Am. Chem. Soc.* **98**, 4395 (1976).
11. Y. Sueishi and N. Nishimura, *Bull. Chem. Soc. Jpn.* **59**, 3305 (1986).
12. G. A. Abakumov, E. S. Klimov and G. A. Rasuvaev, *Dokl. Akad. Nauk SSSR* **205**, 1093 (1972).
13. H. M. McConnell, *J. Chem. Phys.* **24**, 633, 764 (1956).
14. H. M. McConnell and H. H. Dearman, *J. Chem. Phys.* **28**, 51 (1958); H. M. McConnell and D. B. Chesnut, *J. Chem. Phys.* **28**, 107 (1958).
15. E. W. Stone and A. M. Maki, *J. Chem. Phys.* **39**, 1635 (1961).
16. P. H. Rieger and G. K. Fraenkel, *J. Chem. Phys.* **39**, 609 (1963).
17. Y. Ikegami, H. Watanabe and S. Seto, *Bull. Chem. Soc. Jpn.* **45**, 2205 (1972).
18. J. Kirkwood, *J. Chem. Phys.* **2**, 351 (1934).